

SUSTAINED AND TRANSIENT MECHANISMS IN HUMAN VISION: TEMPORAL AND SPATIAL PROPERTIES¹

GORDON E. LEGGE

The Physiological Laboratory, University of Cambridge, Cambridge CB2 3EG, England

(Received 26 October 1976; in revised form 1 June 1977)

Abstract—In two experiments, properties of *sustained* and *transient* mechanisms were studied psychophysically. In the first, contrast thresholds were measured for 6 *sinewave gratings* ranging from 0.375 to 12.0 c/deg at 10 durations ranging from 18 to 3000 msec. Thresholds were measured in the presence and absence of high contrast 20 msec gratings which *masked* the onsets and offsets of the signals. At 1.5 c/deg and above, the unmasked thresholds decreased as power functions of duration in two stages, reaching an asymptotic level near 1000 msec. Below 1.5 c/deg, the unmasked threshold became independent of duration beyond 100 msec. At all frequencies, the masked thresholds decreased as power functions of duration to 1000 msec or more, but the curves for 0.375 and 0.75 c/deg never reached the unmasked asymptotic level. In the second experiment, *spatial frequency bandwidths* were obtained for *sinewave gratings* ranging from 0.375 to 12.0 c/deg, by measuring threshold elevation as a function of the spatial frequency of masking gratings. At 3.0, 6.0 and 12.0 c/deg, the bandwidth functions peaked at the signal frequencies and showed medium bandwidth frequency selectivity. Below 1.5 c/deg, the bandwidth functions exhibited broader spatial frequency tuning, were of higher magnitude, and there was a shift in peak masking to frequencies near 1.0–1.5 c/deg which were above the signal frequencies. The results of both experiments are discussed in terms of the sustained/transient dichotomy.

INTRODUCTION

Campbell and Robson (1968) proposed the existence in the human visual system of a set of independent spatial frequency selective mechanisms for the processing of spatially varying luminance distributions. Their proposal has received a great deal of support from a variety of psychophysical and physiological experiments (Campbell, 1974). Notable among these are the observations of the spatial frequency adaptation phenomenon (Pantle and Sekuler, 1968; Blakemore and Campbell, 1969), the apparent size shift after-effect (Blakemore and Sutton, 1969), and critical band masking in vision (Stromeyer and Julesz, 1972). Other investigators have demonstrated that spatial frequency selective mechanisms may be differentially sensitive to other characteristics of the stimulus distribution. These include differential sensitivity to stimulus orientation (Campbell and Kulikowski, 1966; Movshon and Blakemore, 1973), color (Lovegrove and Over, 1972; Sharpe, 1974), drift velocity (Tolhurst, Sharpe and Hart, 1973), and direction of drift velocity (Tolhurst, 1973).

Various techniques have also been used to measure the temporal properties of spatial frequency selective mechanisms. There appear to be two distinct mechanisms termed *sustained* and *transient*, after possible neural processes. The transient mechanisms respond best to rapid temporal changes, whereas the sustained mechanisms respond best to steady or slowly varying stimuli.

Enroth-Cugell and Robson (1966) provided electrophysiological evidence for a classification of cat

retinal ganglion cells in terms of their spatial summation properties. The *X*-cells exhibited linear spatial summation across the antagonistically organized receptive fields, whereas the spatial summation of the *Y*-cells was nonlinear. Hochstein and Shapley (1976a, b) have studied the *X/Y* classification extensively, and have shown it to be a useful way of categorizing cat retinal ganglion cells. Cleland, Dubin and Levick (1971) have classified cat retinal ganglion cells on the basis of their temporal properties as 'sustained' or 'transient'. The sustained and transient cells possess many of the properties of the *X* and *Y* cells respectively. The transient cells were observed to respond only to the onset or offset of a steady test spot, or maintained a constant response level in the presence of a drifting grating pattern. Sustained cells responded continuously to a steady test spot and followed the temporal modulations of the drifting grating. The transient cells responded to drifting gratings of much higher velocity than the sustained cells, thus demonstrating a higher temporal resolution. Both cell types showed selectivity to stimulus size, with optimal response of sustained cells occurring at a higher spatial frequency than for the transient cells. The sustained and transient ganglion cells in the retina of the cat are differentially distributed, with the preponderance of sustained cells lying in or near the area centralis (Cleland, Levick and Sanderson, 1973). However, the differential distribution may be an electrophysiological sampling artifact. Levick (1975) has argued that the sustained and transient cell types may be identified with the morphologically distinguished alpha and beta cells (Boycott and Wässle, 1974) which have the same retinal distributions. Cleland *et al.* (1971) observed that in the retina and the LGN, the axons of sustained cells are more slowly conducting

¹ Send reprint requests to the author at: Department of Psychology University of Minnesota, 75 East River Road, Minneapolis, Minnesota 55455, U.S.A.

than those of transient cells, and thus it may be inferred that information transmitted by the latter will reach the cortex first (Ikeda and Wright, 1972). Ikeda and Wright (1974) classified cells in area 17 of the cat's visual cortex as either sustained or transient, quite independently of the simple/complex classification of Hubel and Wiesel (Ikeda and Wright, 1975). They found that spatial frequency tuning curves for the sustained cortical cells peak at higher spatial frequencies and have a narrower bandwidth than those for transient cortical cells.

There is evidence that a similar classification can be applied to the primate visual system. Gouras (1969) has shown that transient (termed 'phasic') retinal ganglion cells in the monkey have faster conducting axons than sustained cells (termed 'tonic'). Scobey and Horowitz (1976) have also classified retinal ganglion cells in the monkey as phasic or tonic. The former respond with bursts of action potentials lasting no more than 100 msec following an increment in a luminous test spot, and respond well to bars moved at high velocity across the cell's receptive field. Sherman *et al.* (1976) identified X- and Y-cells in the dorsal LGN of the owl monkey. X-cells exhibited sustained response to stationary patterns, but Y-cells responded for less than 1–2 sec. Y-cells had larger receptive fields and shorter latency to orthodromic stimulation from the optic chiasm than X-cells. Whereas Gouras (1969) found sustained ganglion cells to be color opponent, and transient cells nonopponent, Marrocco (1976) found both sustained and transient cells among opponent and nonopponent LGN cells of macaques. He also found that LGN transient cells have higher conduction velocities than LGN sustained cells, and that nonopponent units had higher conduction velocities than opponent units.

In parallel with the electrophysiological findings, 5 types of psychophysical experiments have provided evidence for sustained and transient mechanisms in human vision.

1. Distinct thresholds for perceiving temporal and spatial modulation

Several investigators have reported that subjects can distinguish phenomenologically between thresholds for temporal variation (flicker), and thresholds for spatial variation (pattern). The two thresholds are independent functions of temporal and spatial frequency (van Nes *et al.* 1967; Keeseey, 1972; Kulikowski and Tolhurst, 1973; Tolhurst, Sharpe and Hart, 1973; King-Smith and Kulikowski, 1975). Flicker sensitivity is ascribed to a transient mechanism because it has a low-pass spatial frequency sensitivity and band-pass temporal frequency sensitivity (Kulikowski and Tolhurst, 1973). Pattern sensitivity is ascribed to a sustained mechanism, because it has a band-pass spatial frequency sensitivity and a peak at lower temporal frequencies. The flicker mechanism would be expected to respond best to coarse gratings switched on and off, and the pattern mechanism to finer gratings of prolonged exposure.

2. Subthreshold summation experiments

Tolhurst (1975b) measured the detectability of a 4 msec grating superimposed upon an 800 msec subthreshold grating of the same spatial frequency. Below 2.0 c/deg, the detectability of the test flash was affected for only 100 msec following onset or offset of the background grating. At higher spatial frequencies, the subthreshold grating increased the detectability of the test flash for the entire

800 msec, suggesting that sustained mechanisms were detecting the grating. King-Smith and Kulikowski (1975) examined the effects on both flicker and pattern thresholds of subthreshold flickering lines and gratings. The flicker detecting mechanisms exhibit nonlinear spatial summation, show weak surround inhibition, and hence are sensitive to low spatial frequencies and even to flickering uniform fields. Pattern detecting mechanisms show linear spatial summation, and comparatively strong surround inhibition. These properties closely parallel receptive field properties of the sustained and transient neurons of the cat's visual system (Ikeda and Wright, 1972).

3. Response latency experiments

Breitmeyer (1975), Vassilev and Mitov (1976), and Lupp, Hauske and Wolf (1976) observed that reaction times for the detection of high spatial frequency gratings are longer than for low spatial frequency gratings, and suggested that the high spatial frequency sensitivity is mediated by sustained neurons with slow conduction velocities. Suprathreshold reaction time experiments, however, are complicated by the fact that increasing contrast leads to a decrease in reaction time. Thus, much of the observed difference in reaction times may be due to differential contrast sensitivity at low and high spatial frequencies. Moreover, Mansfield (1973b) has shown that the reaction time to the onset of a luminous spot can be separated into two components, one dependent on stimulus intensity, and both dependent on target size. Accordingly, the latency differences in the aforementioned studies are difficult to interpret.

4. Thresholds for different temporal waveforms

Several investigators have shown that the waveform of the temporal transients is important to the detection of low spatial frequency targets but not high spatial frequency targets. Kulikowski (1971), and Kulikowski and Tolhurst (1973) have compared contrast thresholds for gratings in counterphase flicker with gratings presented in a periodic on-off mode. The luminance step at a given point for the former is twice that for the latter. Below 2.5 c/deg, sensitivity for the counterphase stimuli was twice that for the on-off stimuli, but above 6.0 c/deg, the two thresholds coincided. Breitmeyer and Julesz (1975) measured the threshold for 500 msec sinusoidal gratings having either gradual or abrupt onsets and offsets. For low spatial frequencies, gratings with an abrupt onset were 50–100% more detectable than gratings with a gradual onset. At high spatial frequencies, the waveform of the transients had no effect on threshold. Tolhurst (1975a) measured reaction times to near-threshold sinusoidal gratings having gradual or abrupt onsets and offsets. At 0.2 c/deg, reaction times were clustered soon after an abrupt onset or offset. If neither onset nor offset were abrupt, thresholds were greatly elevated. Above 1.0 c/deg, the distribution of reaction times was independent of the temporal waveform of the transients.

5. Spatial frequency thresholds as a function of signal duration

Threshold contrast for transient mechanisms should be independent of signal duration, beyond some critical duration which is characteristic of the temporal integration period of the mechanism. (Any realizable system for detecting temporal changes must have a finite temporal resolution and, accordingly, a period of temporal integration). Assuming a stochastically determined threshold, sustained mechanisms may reach threshold at any time during the signal presentation. Therefore, it would be expected that thresholds for sustained mechanisms should continue to drop indefinitely as a function of signal duration. However, the precise shape of the threshold curve will depend upon

the temporal integration of the mechanism and probability summation.

Data on the shape of the threshold curve are limited or equivocal. Nachmias (1967) measured contrast thresholds as a function of signal duration for square wave gratings of spatial frequency 0.7 and 17.5 c/deg. and durations ranging from 11 to 500 msec. At 0.7 c/deg. threshold contrast stopped decreasing after 50–100 msec, but at 17.5 c/deg. threshold contrast was still dropping at 500 msec. In the context of the sustained/transient dichotomy, the interpretation of these results is complicated by the fact that even low frequency square waves have high spatial frequency components. Spitzberg and Richards (1975) compared threshold contrasts of 1000 and 20 msec sinewave grating stimuli at spatial frequencies ranging from 0.15 to 20 c/deg. Below 0.5 c/deg. threshold contrast only doubled, but at 10 c/deg. threshold was raised by a factor of 10. Tulunay-Keesey and Jones (1976) determined threshold contrast as a function of signal duration for sinewave grating stimuli with spatial frequencies of 1.5, 3.0, and 10.0 c/deg. In every case, threshold contrast continued to drop to at least 1000 msec. Unlike Nachmias (1967) and Spitzberg and Richards (1975), they found no significant effect of spatial frequency. However, the lowest spatial frequency, 1.5 c/deg. may not be low enough to reveal the transient mechanisms. Breitmeyer and Ganz (1977) measured contrast thresholds for vertical sinewave gratings with spatial frequencies of 0.5, 2.8, and 16.0 c/deg. for durations of 20–400 msec. The two subjects viewed a field of 17.0 cd/m² mean luminance, subtending 4 × 6°, and made 10 threshold settings for each stimulus. At each spatial frequency, the threshold dropped regularly with time to some critical duration the value of which increased monotonically up to 200 msec at 16.0 c/deg. Beyond the critical duration, there was no further systematic decline in threshold, although the range of durations used may have been insufficient to demonstrate one. Their results indicate no clear qualitative dichotomy between low and high spatial frequencies, but only a progressive shift in the value of the critical duration. Brown and Black (1976) measured threshold luminance for constant contrast square wave gratings on a steady adaptive field. The targets subtended 1° and were presented 2.5° from the fovea. For all gratings of 2–10 c/deg. threshold decreased with duration, up to a critical duration that was as great as 380 msec, whereupon it declined no further. The dependence of critical duration on spatial frequency was non-monotonic, reaching a maximum for an intermediate frequency, the value of which depended upon adapting level.

Only the data of Nachmias (1967) and Spitzberg and Richards (1975) conform with the notion that transient mechanisms detect gratings at low spatial frequencies and sustained mechanisms detect gratings at high spatial frequencies. Their data, although limited to only two spatial frequencies in the case of Nachmias (1967), and only two durations in the case of Spitzberg and Richards (1975), suggest a dichotomy in the shape of threshold curves at low and high spatial frequencies.

Evidence from the five types of psychophysical studies suggests that sinewave grating detection below 1–2 c/deg is mediated by transient mechanisms, and that grating detection at higher spatial frequencies is mediated by sustained mechanisms. The evidence, in some cases, is equivocal (experiments measuring response latency and threshold as a function of signal duration). In others, it is based upon phenomenological reports (ficher vs pattern threshold), or upon the interpretation of experiments with multiple gratings (subthreshold summation experiments) or complicated waveforms.

The present study

The simplest and most direct way of demonstrating the operation of transient and sustained mechanisms at low and high spatial frequencies is to examine the shapes of curves relating contrast threshold to duration. The defining properties of sustained and transient mechanisms should be reflected by qualitative differences in their threshold curves, as discussed in (5) above. In view of the equivocal evidence, cited above, a principal objective of the present study was the measurement of contrast thresholds as a function of the duration of sinewave gratings over a range of signal durations and spatial frequencies that might be expected to demonstrate both sustained and transient mechanisms. Threshold curves were also measured in the presence of brief masking pulses. These were 20 msec presentations of high contrast gratings, identical to the signal, that immediately preceded and followed it (see Fig. 1). For signal detection by a transient mechanism, the shapes of the unmasked and masked threshold curves should be the same, with the masking pulses acting only as 'background transients' to which the signal transients are added. For signal detection by a sustained mechanism, masking should strongly elevate the threshold curve for short durations, but the masked threshold should drop, and approach the unmasked threshold as signal duration increases. Changes in the shape of the threshold curve due to masking, therefore, provide a second test for the operation of sustained and transient mechanisms.

In a second experiment, the transient masking technique was also used to measure spatial frequency bandwidths.

METHOD

Apparatus

Vertical sinewave gratings were generated on a Tektronix 502 oscilloscope with a P2 bluish-green phosphor by means of Z-axis modulation (Campbell and Green, 1965). The luminance of the display was kept constant at 4.6 cd/m². The contrast of the gratings, $(L_{\min} - L_{\max}) / (L_{\min} + L_{\max})$, was kept below 0.30. Above 0.30, sinewave gratings exhibited nonlinear distortion.

Two independent sinewave voltages could be superimposed and applied to the oscilloscope. Each was produced by an Intercil 5038 function generator. The frequency and amplitude of the signals were controlled by a PDP-4 computer via Precision Monolithics DAC-08 D/A converters. Patterns consisting of the superposition of two sinewave modulations, each with adjustable spatial frequency and contrast, were generated at a frame rate of 1/msec. Timing was accurately controlled by a 1 kHz crystal clock in the computer. The contrast of one of these signals could be controlled by a hand held potentiometer. Measurements with a United Detector Technology 80X Opto-meter indicated that the phosphor decayed to 50% in less than 1 msec and had a rise time of less than 1 msec.

The display subtended an angle of 10° in dia. from a viewing distance of 57 cm. (For the measurement of bandwidths at 12.0 c/deg, a viewing distance of 114 cm was used.) The display had a dark surround. The uniformity of the display was checked using a Pritchard Spectra Spot photometer. The function relating contrast to Z-axis voltage and frequency was measured with a scanning slit and photometer. A small, black fixation point was placed at

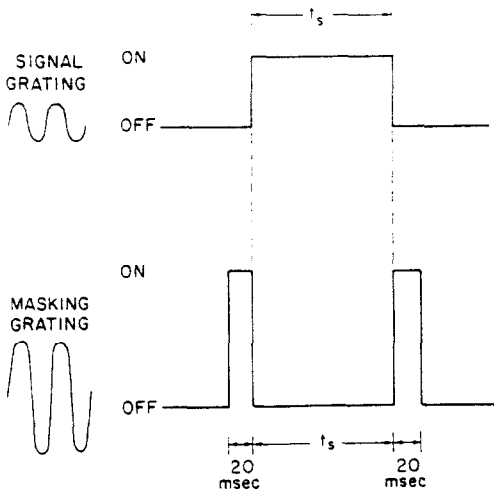


Fig. 1. Temporal waveforms of stimuli. The signal grating was presented for a duration t_s . When present, the masking grating was presented for 20 msec preceding and following the signal. In the first experiment, signal and mask were always at the same spatial frequency. In the second experiment, the frequency of the mask was varied relative to the frequency of the signal.

the center of the display. Subjects viewed the display binocularly with their heads supported by a chin rest. The computer sequenced stimulus presentations and collected data.

Experimental procedure

Each experimental session began with 5 to 10 minutes light adaptation to the uniform display. Threshold estimates were determined by a version of the 2-alternative forced choice procedure (Wetherill and Levitt, 1964). The subject first adjusted the signal contrast to a level just above threshold by turning the potentiometer. The subject was then given a block of trials. Each trial consisted of two presentation intervals, each preceded by 750 msec of the homogeneous screen. Each interval was signalled by a tone, but only one interval contained the test signal. The subject identified the signal interval by pressing one of two keys, thereby initiating the next trial. A correct decision was followed by a tone. Two consecutive correct decisions at a given contrast level were followed by a constant decrement in contrast, and one incorrect decision was followed by an increment of the same size. (Prior to the first incorrect decision, all correct decisions were followed by the constant decrement.) The mean of the contrast peaks and valleys in the resulting sequence provides an estimate of the 71% frequency-of-seeing level (Wetherill and Levitt, 1964). There were 55 trials per block used to obtain the first threshold estimate under a given set of stimulus conditions, and 40 per block for subsequent determinations. Typically, at least 4 pairs of peaks and valleys were contained within each block. The threshold measure was the geometric mean of these estimates. The error bars in Figs. 3, 5 and 6 correspond to ± 1 standard error of the means. The geometric mean was used because the corresponding errors appeared to be roughly constant in logarithmic units. Prior to averaging, slight day-to-day and subject-subject variations in overall sensitivity were cancelled by normalizing threshold estimates from a given session by the geometric mean of all estimates taken. After averaging, data were rescaled by the grand mean.

In the first experiment, contrast thresholds were measured as a function of stimulus duration. Within a session, threshold estimates for one of 6 spatial frequencies

(0.375, 0.75, 1.5, 3.0, 6.0 and 12.0 c/deg) were obtained at each of 8 durations (13, 30, 56, 100, 180, 300, 560 and 1000 msec), with and without transient masks. The transient masks were identical to the test grating but of contrast 0.22, and preceded and followed the test grating for 20 msec (see Fig. 1). Three threshold estimates were obtained for each subject under each condition. In separate sessions, otherwise identical measurements were made for the 6 spatial frequencies, and signal durations of 1000, 1800 and 3000 msec. (Unmasked thresholds at 0.375 and 0.75 c/deg were not measured beyond 1000 msec because the curves were already independent of duration.)

In a second experiment, brief masking stimuli were used to measure the spatial frequency bandwidths of transient responses at spatial frequencies of 0.375, 0.75, 1.5, 3.0, 6.0 and 12.0 c/deg. Thresholds for 100 msec signals of constant spatial frequency were measured as a function of the spatial frequency of the masking pulses extending at least ± 1 octave from the test frequency. Each session was devoted to a single test frequency. For each subject, 4 threshold estimates were obtained for bandwidth functions at 0.375 and 0.75 c/deg, and 2 for the other 4 spatial frequencies.

Subjects

There were two subjects, both highly practiced with the methods and stimuli, but both naive to the specific purposes of the experiments. JD, an optically corrected myope (right eye, -8.0 D; left eye, -7.25 D), is a male in his early twenties. WWL, an optically corrected astigmat (right eye, -1.25 D at 135°; left eye, -1.75 D at 15°), is a female in her early twenties. Figure 2 shows contrast sensitivity functions for the two subjects. The individual differences are small, apart from an overall decrease in sensitivity for JD. Such a decrease is typical of myopic subjects (Fiorentini and Maffei, 1976). Both subjects have normal color vision.

RESULTS AND DISCUSSION

Contrast threshold as a function of signal duration

Figure 3 presents contrast thresholds as a function of signal duration for sinewave gratings of 6 spatial frequencies in the absence of masking. To facilitate their display, sets of data have been vertically dis-

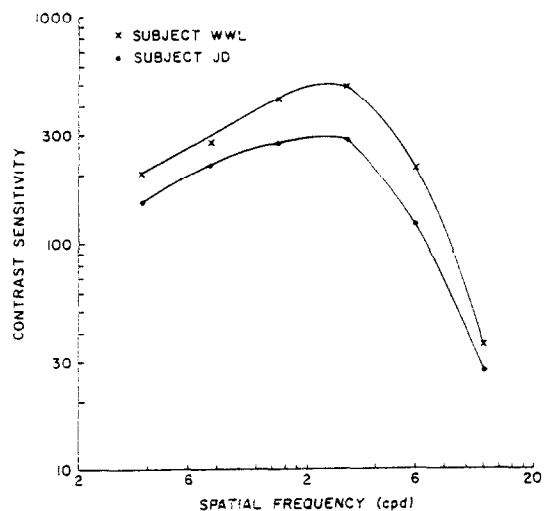


Fig. 2. Contrast sensitivity functions. (x): Subject WWL; (●): Subject JD. Each data point is the geometric mean of 5 threshold estimates, each derived from a block of forced choice trials. Smooth curves have been drawn through the data. Signal duration = 100 msec. The standard errors were always less than 15%.

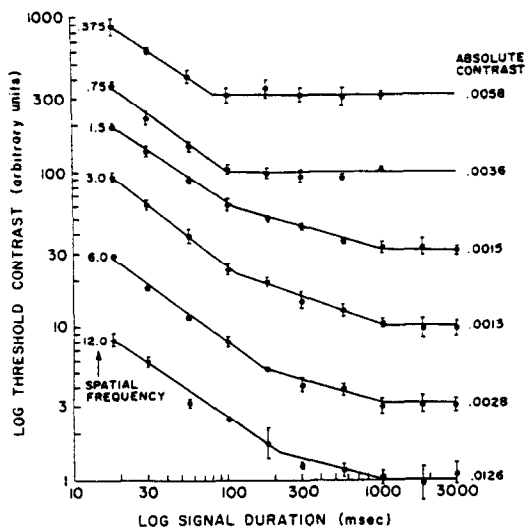


Fig. 3. Threshold as a function of duration. Contrast thresholds are plotted as a function of signal duration for 6 spatial frequencies. To facilitate display, the sets of data points have been vertically displaced and sequenced in order of spatial frequency. The ordinate values give the relative contrasts for points within a set. Absolute contrast of the asymptotic level of each curve is given at its right. Data points are the geometric means of 6 threshold estimates (18–1000 msec) or 4 estimates (1800 and 3000 msec) from 2 subjects. Threshold estimates were obtained from blocks of forced choice trials. Error bars represent ± 1 s.e. Each set of data has been fitted piecewise with straight line segments (see Table 1).

placed relative to each other. Accordingly, ordinate values are strictly relative. The absolute contrasts of the asymptotic levels of each curve are shown at the right. The data points are geometric means of 6 threshold estimates (for 18–1000 msec), or 4 estimates (1800 and 3000 msec), from two subjects. An estimate was obtained from a block of forced choice trials (see Method). Accordingly, each point was based upon approximately 270 trials, and each curve upon approximately 2300 trials. Error bars represent ± 1 standard error of the means. There were no apparent differences in the shapes of the threshold functions between subjects.

At spatial frequencies of 1.5 c/deg and above, threshold continued to decrease to 1000 msec. The general features of the threshold curves are similar, and are as predicted for sustained mechanisms. There was a brief, fairly steep threshold decrease, due to temporal integration, followed by a longer, secondary decline presumably due to probability summation. An asymptotic level was reached, near 1000 msec, after which threshold became independent of duration. Both segments of the declining portions of the threshold curves can be approximated by straight lines (fit by least squares) in the double-logarithmic coordinates. The intersection of these two lines, conventionally called the *critical duration*, increases with spatial frequency, reaching 215 msec at 12.0 c/deg.

At 0.375 and 0.75 c/deg, there was a brief threshold decrease after which threshold became independent of time. The independence of threshold and signal duration beyond some critical duration is a character-

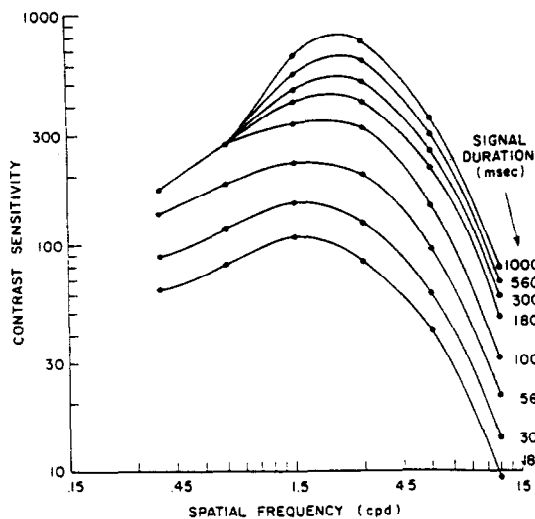


Fig. 4. Contrast sensitivity functions for different signal durations. Values from the best fitting straight lines through the data in Fig. 3 have been replotted as contrast sensitivity, the reciprocal of threshold contrast, as a function of spatial frequency. Smooth curves have been drawn through the points. The 8 sets of data are for the signal durations, in msec, as indicated. The convergence of the curves for 100 msec and longer at low spatial frequencies is a consequence of the transient nature of low spatial frequency response.

istic attributable to a mechanism with transient response.

The threshold contrasts of Fig. 3 are replotted in Fig. 4 as a function of spatial frequency. The ordinate is contrast sensitivity, the reciprocal of threshold contrast, and 8 signal durations are parameters. The filled circles are values taken from the fitted straight lines in Fig. 3. Smooth curves have been drawn through them. Notice the growth of the medium frequency sensitivity peak and its rightward shift with increasing duration, also observed by Schober and Hilz (1965), and Nachmias (1967).

Figure 5 presents contrast thresholds as a function of signal duration for the same 6 sinewave gratings, in the presence of brief, masking gratings. The masking gratings were identical to the signal gratings, but of contrast 0.22, and were presented for 20 msec immediately before and after the signal. The data were processed in the same manner as the unmasked data of Fig. 3, and are presented in a similar format. The dashed lines, labelled by absolute contrast values, are the asymptotic levels of the unmasked threshold curves of Fig. 3. The best fitting straight lines through the data have been drawn.

For signals of 1.5 c/deg and above, the shape of the masked threshold curves conforms with predictions made for sustained mechanisms. There was a pronounced increase in threshold for short times, but as signal duration increased, the masked threshold curve converged with the unmasked curve.

For signals of 0.375 and 0.75 c/deg, the unmasked threshold curves show a steady decline to about 1000 msec, whereupon they level out at contrasts well above the asymptotic value of the unmasked signals. For transient mechanisms, it was predicted that masking should simply elevate the threshold curves,

leaving their shapes invariant. Comparison of Figs. 3 and 5 shows that this is not the case for the threshold curves at 0.375 and 0.75 c/deg. Compared with the independence of threshold for duration beyond 100 msec for the unmasked curves, the steady decline to 1000 msec of the masked curves is a feature more characteristic of sustained response. It is therefore postulated that the masking procedure has elevated the transient threshold curve above the threshold curve for a coexisting sustained mechanism. In the absence of masking, the transient mechanism is more sensitive and its presence is revealed by measurements of threshold as a function of duration. In the presence of masking, the transient mechanism is less sensitive and properties of the sustained mechanism are revealed by threshold measurements. Notice also that the asymptotic levels of the masked curves, beyond 1000 msec, are a factor of 2 higher in threshold than the unmasked curves. This result may be interpreted as indicating that the asymptotic threshold of the coexisting sustained mechanism is higher than the asymptotic threshold for the unmasked transient mechanisms.

If transient mechanisms and less sensitive sustained mechanisms both operate in the detection of low frequency gratings, low contrast masking that only slightly desensitizes a transient mechanism should elevate the threshold curve, but leave its shape invariant. Investigations of this point indicated that masks of contrast less than 0.10 had little or no effect on the threshold curve at 0.375 c/deg. In Fig. 6, the threshold curve for masking with contrast 0.11 is shown, together with data replotted from Figs. 3 and 5 for no masking, and masking contrast of 0.22, re-

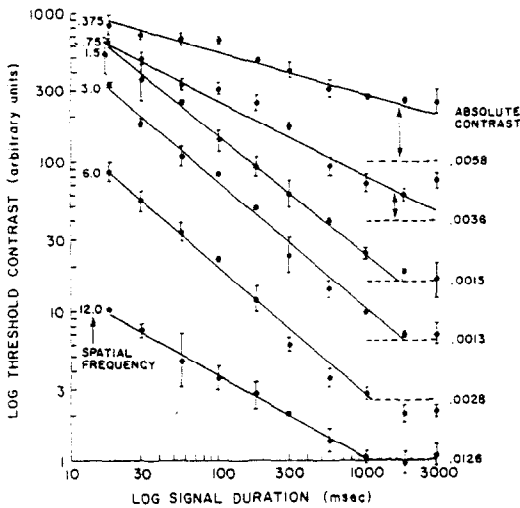


Fig. 5. Masked threshold as a function of duration. Contrast thresholds are plotted as a function of signal duration for 6 spatial frequencies in the presence of masking. The mask was a sine wave grating identical to the signal, but of contrast 0.22. It was presented for 20 msec immediately preceding and following the signal. In the figure, sets of data points have been vertically displaced, and sequenced in order of spatial frequency. The ordinate values give the relative contrast for points within a set. The dashed lines give the asymptotic levels for the unmasked curves (see Fig. 3) at the same spatial frequency. Each set of data has been fitted by a straight line (see Table 1). Other details of the data are as described for Fig. 3.

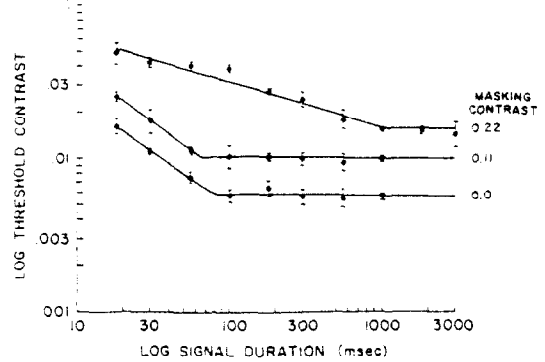


Fig. 6. Contrast thresholds are plotted as a function of duration for 0.375 c/deg signals with 3 levels of masking. Data for masking contrasts of 0.0 and 0.22 are replotted from Figs. 3 and 5 respectively. For the masking contrast of 0.11, data points are geometric means of 4 threshold estimates, 2 each from 2 subjects. Each estimate was obtained from a block of forced choice trials. The straight line, fitted to the first 3 points, has a slope of -0.72 .

spectively. Data points for the intermediate curve were based on 4 forced choice threshold estimates (see Method), 2 from each subject. The major effect of masking with contrast 0.11 was to elevate the unmasked threshold curve, while maintaining the main features of its shape. This result strengthens the interpretation of the low frequency masked threshold curves given above.

Taken together, both the unmasked and the masked data of Figs. 3 and 5 argue for the functioning of sustained mechanisms at high spatial frequencies. At low spatial frequencies, the unmasked data argue for the functioning of transient mechanisms, but the masked threshold data require a more complicated interpretation.

Table 1 lists the slopes of the straight lines used to fit the data of Figs. 3 and 5, together with the critical durations determined from the unmasked curves. The ranges of duration in which the regression lines were fit are shown, as well as the standard error of the slopes (formula for the standard error given by Mansfield 1973b). Notice that the slopes of the initial straight lines are nearly the same at all spatial frequencies, mean = -0.72 . This value is in agreement with the value of -0.70 found by Breitmeyer and Ganz (1977) and with comparable data of Nachmias (1967), but is smaller than the values, -0.82 to -0.94 , found by Tulunay-Keesey and Jones (1976). The similarity of slopes over the wide range of spatial frequencies, including both transient and sustained mechanisms, presumably reflects a uniformity of the physiological mechanism of temporal integration. However, note that the extent of temporal integration, as indexed by the critical duration, increases from 81 msec at 0.375 c/deg to 215 msec at 12.0 c/deg. Beyond the critical duration, the low frequency thresholds are independent of signal duration (virtually 0 slope), but the high frequency thresholds decline with slopes near -0.30 . The latter are in agreement with the measurements of Tulunay-Keesey and Jones (1976).

Table 1 also gives the slopes of the straight lines used to approximate the masked thresholds. Notice that the slopes are similar for the sustained mechan-

Table 1. Threshold as a function of duration: parameters

| Spatial frequency (c/deg) | Unmasked | | | | | Masked | |
|---------------------------|---------------------|---------------|---------------------|-----------------|-------------------|---------------------|--------------|
| | Fitted range (msec) | Initial slope | Fitted range (msec) | Secondary slope | Critical duration | Fitted range (msec) | Slope |
| 0.375 | 18-56 | -0.67 ± 0.04 | 100-1000 | -0.03 ± 0.04 | 81 | 18-1000 | -0.29 ± 0.03 |
| 0.75 | 18-100 | -0.72 ± 0.06 | 100-1000 | -0.02 ± 0.04 | 100 | 18-1800 | -0.51 ± 0.04 |
| 1.5 | 18-100 | -0.67 ± 0.02 | 100-1000 | -0.27 ± 0.02 | 112 | 18-1000 | -0.80 ± 0.02 |
| 3.0 | 18-100 | -0.80 ± 0.03 | 180-1000 | -0.34 ± 0.05 | 111 | 18-1800 | -0.80 ± 0.09 |
| 6.0 | 18-180 | -0.74 ± 0.04 | 180-1000 | -0.29 ± 0.04 | 167 | 18-1800 | -0.86 ± 0.04 |
| 12.0 | 18-180 | -0.68 ± 0.05 | 180-1000 | -0.26 ± 0.09 | 215 | 18-1000 | -0.56 ± 0.02 |

isms at 1.5, 3.0 and 6.0 cpd, but considerably less for the putative sustained mechanisms revealed by transient masking at 0.75 and 0.375 c/deg. A tentative explanation for the difference is given below, in the discussion of the bandwidth measurements.

Threshold as a function of duration for acuity targets and spot detection

A qualitative dichotomy in the form of the contrast threshold versus duration curves at high and low spatial frequencies is paralleled by a dichotomy in the older contrast detection literature. Measures of the absolute or increment detection thresholds of luminous spots yield threshold curves analogous to those of transient detection, whereas acuity tasks, depending on the detection of patterned features, yield threshold curves analogous to those for sustained detection.

Bloch's Law states that, for the detection of luminous spots, there is a period of complete reciprocity between threshold luminance and time:

$$Lt = k, \quad t < t_c$$

where L is luminance, t time, k a constant, and t_c a critical duration. Graham and Kemp (1938) have shown that Bloch's Law holds for the detection of foveal brightness increments. They have shown that the critical duration decreases with increasing adapting level, ranging from 100 msec at 0.006 cd/m² to 30 msec at 550 cd/m². Beyond the critical duration, they observed an abrupt transition to threshold independent of duration. Both Blackwell (1963) and Barlow (1958), also observed the decrease in critical duration with increasing adapting luminance but noted a more gradual transition from Bloch's Law to the independence of threshold and duration. Barlow (1958) observed that the threshold decline continued over much longer durations for small spots, 0.01 deg² area, than for large spots, 27.6 deg² area. A suprathreshold version of Bloch's Law also holds. Mansfield (1973a) has shown that, for small test targets, equal brightness judgments are governed by a reciprocal relation between stimulus luminance and duration.

In double-logarithmic coordinates, Bloch's Law implies a straight line relationship between threshold luminance and stimulus duration, with a slope of -1.0. Table 1 illustrates that the threshold curves of Fig. 3 have initial slopes ranging from -0.67 to -0.80. It is hard to account for the discrepancy in slope values for spot detection and grating detection experiments. It may be related to target size. Grating detection experiments typically use targets of several degrees subtense. Mansfield (1973a) has shown that, for targets larger than some critical area, the suprathreshold version of Bloch's Law breaks down, even for the briefest test flashes. The same may be true for threshold detection of gratings. Note that the slope values obtained with grating targets are closer to the value of -0.5, the value to be expected for ideal, quantum-limited detection (Barlow, 1958), than are the slopes for spot detection.

For the detection of acuity targets, threshold as a function of duration curves are found to drop for durations much longer than those observed for spot detection. Kahneman (1964) studied the visibility of Landolt C's. At photopic levels, critical durations extended from 350 to 1000 msec, for increasing intensity-time products. Baron and Westheimer (1973) examined acuity for the critical feature of a Landolt C as a function of exposure duration. From their Fig. 2, it is clear that acuity continues to improve for durations of at least 400 msec, and perhaps as long as 1000 msec. With the use of an artificial pupil and a cycloplegic, pupillary and accommodative fluctuations were shown not to be the determinants of the shape of the threshold curve.

The differences in the duration of threshold decrease for acuity and spot detection tasks may be partially accounted for if acuity targets (such as Landolt C's or grating stimuli) are assumed to be more highly patterned than large luminous spots—that is, if the former differentially stimulate mechanisms sensitive to fine detail. Kelly (1971) has commented that in the context of his theory of flicker detection, circular spot stimuli represent an intermediate case between patterned grating stimuli and nonpatterned uniform fields with respect to spatio-temporal sensitivity. If this be so, then detection of acuity targets may be due to the operation of sustained mechanisms with their characteristic threshold curves, and the detection of large spot stimuli may often be accomplished by transient mechanisms with their characteristic threshold curves.

Eye movements

It has been argued (Arend, 1976a; b) that the dichotomy in the form of threshold versus duration curves at low and high spatial frequencies may be due to the increased effect of eye movements upon the latter. In the present study, subjects were instructed to fixate a small, black dot at the center of the display. Under these conditions, median eye movements during 250 msec exposures are less than 1', and for 1000 msec exposures, they are 3.2' (Riggs, Armington and Ratliff, 1954). Such eye movements would not be expected to greatly influence the detection of 1.5 c/deg gratings, for which 1 cycle subtends 40' of visual angle. Since the threshold curve for 1.5 c/deg is like those for higher spatial frequencies, and qualitatively different from those at lower spatial frequencies (see Fig. 3), the difference does not appear to be due to eye movement. Moreover, experiments with stabilized images indicate that eye movements play little role. Keesey (1960) has demonstrated that the prolonged decline of threshold as a function of duration for acuity targets occurs with or without stabilization. Tulunay-Keesey and Jones (1976) have shown that threshold curves for sinusoidal gratings with spatial frequencies up to at least 10 c/deg decrease to 1000 msec with or without stabilization.

Threshold as a function of duration: temporal integration and probability integration

In Table 1, values for the slopes of the unmasked thresh-

old vs duration curves of Fig. 3 are given. At all spatial frequencies, the initial slope is close to -0.7 . For the sustained mechanisms, 1.5 c/deg and above, the subsequent slopes are close to -0.3 . These values may result from effects of temporal integration and probability integration.

Both *temporal integration* and *probability integration* are inherent in the concept of a sustained mechanism. The former reflects the finite temporal resolution of the mechanism. The latter represents the increasing probability with increasing duration that a threshold level will be achieved, given the variable nature of the mechanism's response. Both types of integration contribute to a decline in threshold with increasing duration.

Let the response R of a detecting mechanism be proportional to the convolution of the signal contrast $C(t)$ and a temporal integration profile $w(t)$:

$$R(t) = \int_{-x}^t C(T)w(t-T) dT \quad (1)$$

Assume that $w(t)$ has the form:

$$w(t) = \begin{cases} 0, & t < 0 \\ t^{-m}, & 0 < t < t_0 \\ 0, & t > t_0 \end{cases} \quad (2)$$

where t_0 is a cutoff, or *critical duration*. For a steady signal of contrast C_0 , turned on at $t = 0$, equations (1) and (2) yield the following response function:

$$R(t) = \begin{cases} \frac{1}{1-m} C_0 t^{1-m}, & t < t_0 \\ \frac{1}{1-m} C_0 t_0^{1-m}, & t > t_0 \end{cases} \quad (3)$$

It is assumed that if a detector's response exceeds threshold at any time during the signal interval, a 'detect' state occurs, and the subject will report seeing the stimulus. The false alarm rate is assumed to be negligible. It is further assumed that a threshold response is stochastically determined, and that the form of the probability-of-seeing density function is:

$$f(t) = 1 - e^{-\alpha R(t)^\beta} \quad (4)$$

where α and β are constants. $f(t)$ is called a density function because it represents the probability-of-seeing per unit time. Green and Luce (1975) have shown that this form

is the only one which preserves its shape under translation along the log contrast axis for the type of probability integration assumed here. Since probability-of-seeing curves obtained with different exposure durations have this invariance property (Nachmias, 1967), and for computational convenience, this form has been adopted. The constant α is a scaling parameter and β determines the steepness of the probability-of-seeing curve. The probability of 'seeing' a stimulus presented for time t_r is:

$$P_{see} = 1 - \exp \left[- \int_0^{t_r} \ln(1-f(t)) dt \right] \quad (5)$$

A proof of (5) is given in the Appendix. Inserting the density function of (4) and the response function of (3):

$$P_{see} = \begin{cases} 1 - \exp[-k_1 C_0^\beta t_r^{1-m\beta+1}] & t_r < t_0 \\ 1 - \exp\{-C_0^\beta [k_2 + k_3(t_r - t_0)]\} & t_r > t_0 \end{cases} \quad (6)$$

where k_1 , k_2 , and k_3 are constants.

For the experiments reported in this paper, a procedure was used which estimated contrasts for a fixed probability-of-seeing level as a function of signal duration t_r . This occurs when the exponent in (6) remains constant. Consider two cases.

(1) For signal durations t_r very much greater than the integration time t_0 , the preceding condition obtains when:

$$C_0^\beta t_r = \text{const} \quad (7)$$

or:

$$C_0 \propto t_r^{-1/\beta} \quad (8)$$

In log-log coordinates, this relation is represented by a straight line of slope $-1/\beta$. According to Table 1, the secondary decline of the contrast threshold vs duration curves may be represented by straight lines with slopes near -0.3 . Then, according to (8), $\beta \sim 3$. Such a value for β corresponds to a very steep probability-of-seeing curve. However, data from a variety of studies (Blackwell, 1946; Blackwell, 1963; Nachmias, 1967; Sachs, Nachmias and Robson, 1971) report steep probability-of-seeing curves for contrast detection tasks under a wide variety of conditions. Figure 7 presents frequency-of-seeing curves for the detection of 3.0 cpd gratings from the two subjects. The solid curves through the data have the form $1 - 0.5 \exp(-\alpha C^\beta)$ where C is contrast, and $\beta = 2.5$. (The factor 0.5 in the foregoing expression results from the assumption that in trials for which threshold is not

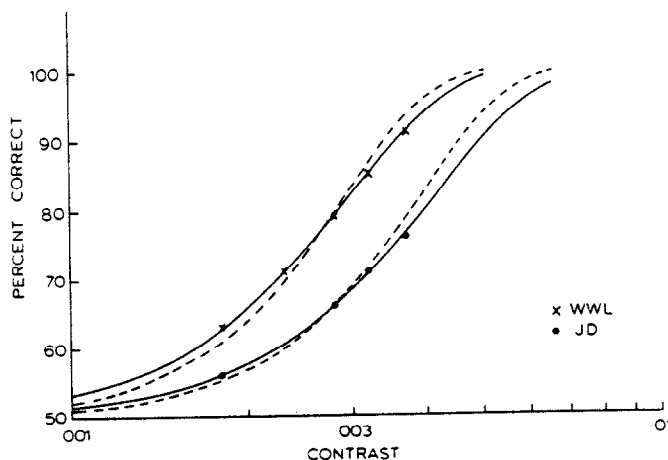


Fig. 7. Frequency-of-seeing functions. (x): Subject WWL; (●): Subject JD. The signal was a 3.0 c/deg grating presented for 180 msec. Each data point is based on 160 forced choice trials, and all data were collected in single sessions. Curves through the data have the form $1 - 0.5 \exp(-\alpha C^\beta)$, where α and β are constants and C is contrast. Solid curve: $\beta = 2.5$; dashed curves: $\beta = 2.94$.

achieved, a subject will guess correctly 50% of the time.) A value of $\beta = 2.94$ is predicted from the reciprocal of the secondary slope for the 3.0 c/deg grating in Fig. 3. The dashed lines in Fig. 7 present the predicted curve. The discrepancy between predicted and observed curves is small, and may be due to some unknown source of variability in the frequency-of-seeing measurements.

(2) For signal durations less than the integration time t_0 , the condition equivalent to equation (7) is:

$$C_0^d t_s^{(1-m)\beta+1} = \text{const} \quad (9)$$

or:

$$C_0 \propto t_s^{-(1-m+1/\beta)} \quad (10)$$

In log-log coordinates this relation is represented by a straight line of slope $1 - m + 1/\beta$. According to Table 1, the initial portions of the threshold curves may be represented by straight lines with slopes near -0.7 . Since $1/\beta$ has been evaluated as 0.30, $m \sim 0.6$. This means that the integration profile $w(t)$ of equation (2) has the form $t^{-0.6}$. This profile weights recent times more heavily than distant ones. For a critical duration of 100 msec, for instance, half of the area of the weighting function is contained within the first 18 msec.

According to the foregoing derivations, the gradual decline in threshold beyond the critical duration is solely due to probability integration and is independent of the character of temporal integration. On the other hand, for durations less than the critical duration, the steeper decline in threshold is due both to the shape of the temporal integration profile and to characteristics of probability integration.

The asymptotic levels reached by the threshold curves beyond 1000 msec indicate that the threshold decline due to probability summation is not unbounded. For long durations, subjects reported some difficulty in maintaining good fixation and accommodation. Factors such as these probably account for the presence of the asymptotic level.

Bandwidth functions obtained with masking

In the second experiment, thresholds for 100 msec signals of a given spatial frequency were measured as a function of the spatial frequency of briefly pres-

ented masking gratings of contrast 0.22. The masking gratings were like those used in the first experiment (see Fig. 1), except that their spatial frequencies varied both above and below the spatial frequency. They acted to preferentially desensitize the transient response of detecting mechanisms.

In Fig. 8, the ratio of masked to unmasked threshold is plotted in decilogs as a function of spatial frequency for signals of 3.0, 6.0 and 12.0 c/deg. The data points are geometric means of 4 threshold estimates, 2 from each subject. An estimate was obtained from a block of forced choice trials (see Method). Smooth curves have been drawn through the data points. There were no systematic differences in the shapes of the bandwidth functions between the two subjects. The shapes of the curves reveal characteristics of the spatial frequency selectivity and peak sensitivity of the mechanisms detecting the specified signals. In each case, the peaks of the bandwidth curves occurred at the signal frequency. The masking was broader at 3.0 c/deg (about 2.0 octaves between half-maximum values). Masking was asymmetrical, being slightly broader below the peak. The decrease in the magnitude of masking from 3.0 to 12.0 c/deg was undoubtedly due to the decreased sensitivity of the visual system to masks of contrast 0.22 at increasing spatial frequencies. The shapes of the bandwidth functions shown in Fig. 8 are in general agreement with the masking functions obtained under quite different conditions by Stromeyer and Julesz (1972). Unlike the present study, they used a procedure in which the frequency of the masking stimuli (1 octave wide bands of noise) were held constant, while the frequencies of the test stimuli were varied. Since they used continuous signal presentations, the similarity in the shapes of the measured bandwidth functions suggest that the spatial frequency selectivity of sustained mechanisms at or above 3.0 c/deg is unchanged for signal durations as brief as 100 msec.

The facilitating effects of masks whose spatial fre-

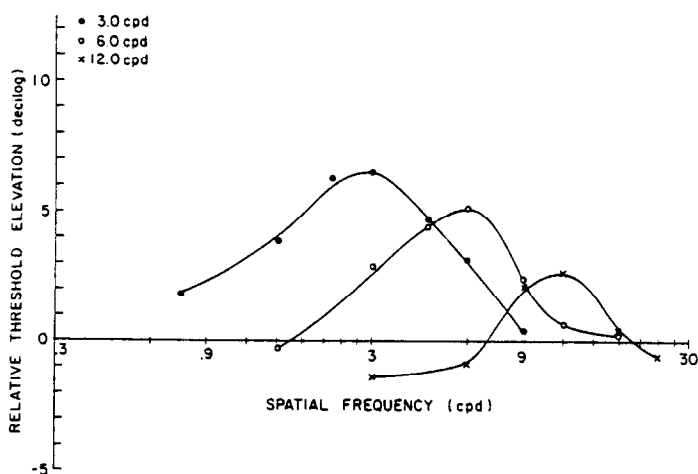


Fig. 8. Bandwidth functions at high spatial frequencies. Contrast thresholds for sinewave grating signals of 3.0, 6.0 and 12.0 cpd have been measured as a function of the spatial frequency of masks. The masks consisted of 20 msec pulses of sinewave gratings immediately preceding and following the signal gratings. The contrast of the mask was 0.22. Duration of the signal was kept constant at 100 msec. The ordinate is the ratio, in decilogs, of the masked threshold contrast to the unmasked threshold contrast of the signal presented for 100 msec. Data points are geometric means of 4 threshold estimates, 2 each from 2 subjects. Each estimate was obtained from a block of forced choice trials. Smooth curves have been drawn through the data. The standard errors were always less than 20%.

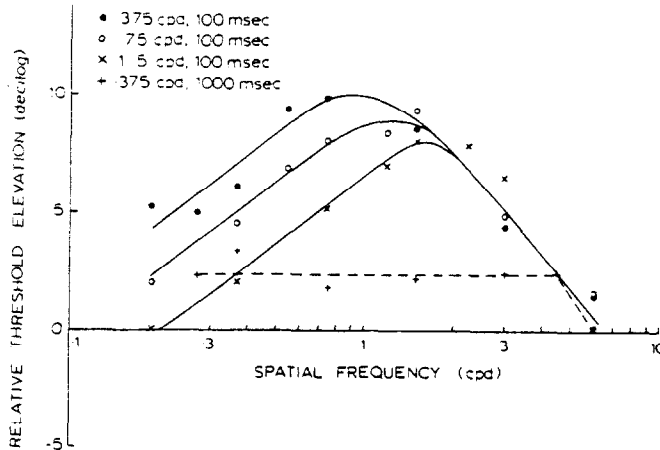


Fig. 9. Bandwidth functions at low spatial frequencies. Contrast thresholds of sinewave grating signals of 0.375 (●), 0.75 (○), and 1.5 (×) cpd, 100 msec duration, have been measured as a function of the spatial frequency of masks. Details are the same as for Fig. 8 except: data points are the geometric means of 8 threshold estimates, 4 from each of 2 subjects. Separate smooth curves have been drawn through the 3 sets of data to the left of 1.5 c/deg, and a single curve through all the data to the right of 1.5 c/deg. The standard errors were always less than 15%. (+) symbols give contrast thresholds for 0.375 c/deg signals of duration 1000 msec as a function of the spatial frequency of masks. They are geometric means of 4 threshold estimates, 2 from each of 2 subjects.

quencies were well below the signal frequency (see the curve for 12.0 c/deg in Fig. 8), have been observed by other investigators under other conditions (Stromeyer and Klein, 1974; Nachmias and Weber, 1975).

In Fig. 9, corresponding bandwidth functions are plotted for signal frequencies of 0.375 (●), 0.75 (○), and 1.5 (×) cpd. (The + symbols will be discussed below.) Each data point is the geometric mean of 8 threshold estimates, 4 from each subject. Smooth curves have been drawn through the data. The bandwidth functions grew broader for signals of decreasing spatial frequency. The increasing breadth was chiefly manifested by a separation of the curves below 1.5 c/deg. This separation demonstrated the increased effect of low frequency masking upon low frequency signals. To the right of their peaks, the three curves descended together toward zero at higher spatial frequencies. Peak masking at the lowest signal frequency of 0.375 c/deg did not occur at the signal frequency, but was displaced about 1 octave to the right.

In connection with the masked threshold data for 0.375 and 0.75 c/deg in Fig. 5, it was observed that the shapes of the threshold curves indicate the functioning of sustained mechanisms at low spatial frequencies. Two features of the bandwidth data in Fig. 9 suggest that the sustained mechanisms in question have optimal sensitivity near 1.0 c/deg.

(1) The shift in peak masking to an octave above the signal frequency of 0.375 c/deg suggests that the signal was detected by a mechanism with peak sensitivity above 0.375 c/deg.

(2) The vertical separation of the bandwidth functions below 1.5 cpd suggests that detection is mediated by a single mechanism. This is so because the more remote the signal frequency is from the optimal frequency of the detecting mechanisms, the more the former's contrast must be raised before the latter's threshold is reached. (Recall that the transient mechanisms which are responsible for detection under normal conditions have been preferentially desensitized

by the transient masking procedure). According to this interpretation, the convergence of the curves at higher spatial frequencies reflects the recovery of sensitivity by the low frequency transient mechanisms as the masking frequency becomes more remote.

A check on the assumption that the low spatial frequency bandwidth functions reflect characteristics of sustained mechanisms is provided by reference to the (+) symbols in Fig. 9. They give results of an experiment in which bandwidth functions were obtained for 0.375 c/deg signals of 1000 msec duration. The data points (+) are geometric means of 4 threshold estimates, 2 from each subject. The (+) symbols represent the ratios, in decilogs, of masked thresholds for 1000 msec, 0.375 c/deg signals, to unmasked thresholds for 100 msec signals at the same spatial frequency. If threshold detection under conditions of masking were due to sustained mechanisms, the 1000 msec signals would be expected to yield lower thresholds and hence, lower bandwidth functions. As may be seen in the figure, this is the case. The masking functions for 1000 msec presentations are nearly flat up to a spatial frequency of about 4.5 c/deg having an ordinate value near 3 decilogs. This confirms the suggestion that, under conditions of transient masking, a sustained mechanism accounts for the threshold detection of grating signals of spatial frequencies at 0.375 c/deg.

Stated otherwise, the foregoing result implies that masks ranging over at least 4 octaves (0.18 to 3.0 c/deg) preferentially desensitize the transient response at 0.375 cpd. This is consistent with the observations of Kulikowski and Tolhurst (1973) who found that flicker sensitivity has a low-pass spatial frequency sensitivity. The results may further suggest that flicker (transient) response is single channel in character, unlike the multiple channel character of sustained response.

Evidence for the existence of a 'lowest adaptable channel' comes from the work of Blakemore and

Campbell (1969), and Tolhurst (1973). These investigators demonstrated a shift in the peak of spatial frequency adaptation bandwidth functions to frequencies higher than the adapting frequencies. However, they did not demonstrate the expected broadening of the bandwidth functions below the peak, as exhibited in Fig. 9 for the bandwidth functions obtained with masking. Stromeyer *et al.* (1976) demonstrated spatial frequency adaptation with spatial frequencies as low as 0.5 c/deg. In their study, adapting gratings were presented in random phase jitter at a contrast of 0.11 on a display subtending 18°. For adaptation at 0.5 c/deg, there were strong threshold elevations for spatial frequencies 2 octaves below at 0.12 c/deg, suggesting the signals at these low spatial frequencies were being detected by the adaptive channel at 0.5 c/deg. Stromeyer *et al.* (1976), however, did not observe a shift in the peak of the bandwidth functions away from the adapting frequency.

In the discussion concerning Fig. 5, it was observed that the decline in threshold with duration for the masked curves at spatial frequencies of 0.375 and 0.75 c/deg was more gradual than for the sustained mechanisms at higher spatial frequencies. This may have been due to one of the following:

(I) The desensitizing effects of transient masks at 0.375 and 0.75 cpd were small on the 'lowest sustained channel' at 1.5 c/deg, and thus, not as much recovery of sensitivity was possible.

(II) The extent of temporal integration may be less for nonoptimal stimuli—namely, stimuli at 0.375 and 0.75 c/deg being detected by a mechanism with optimal sensitivity at 1.5 c/deg.

Figure 10 schematically summarizes the relations between transient and sustained mechanisms, as inferred from the experiments.

(1) In the absence of masking, threshold behavior is governed by transient mechanisms below 1.0 c/deg,

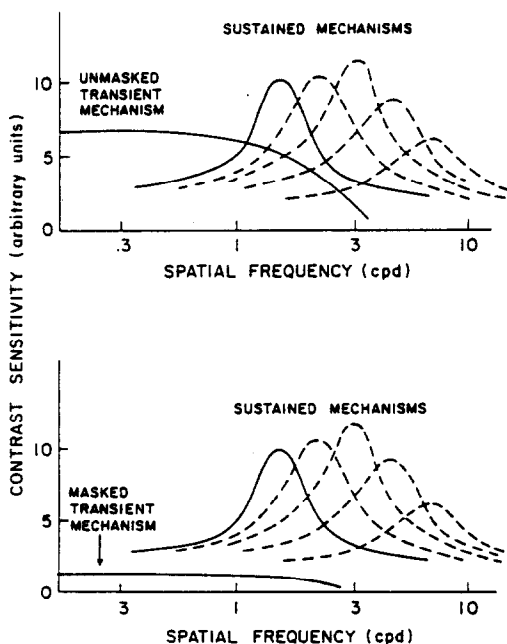


Fig. 10. Schematic diagram of the sensitivity of transient and sustained mechanisms. (a) In the absence of masking; (b) In the presence of masking.

and by sustained mechanisms at higher frequencies (Fig. 3).

(2) Masking indicates that sustained mechanisms are relatively narrowband (Fig. 8), but the transient mechanisms are low-pass and relatively broadband (Fig. 9, + symbols).

(3) There is a lowest sustained channel (Fig. 9). In the presence of transient masking, it has greater sensitivity at frequencies below 1.0 c/deg than does the transient mechanism (Figs. 5 and 9).

SUMMARY AND CONCLUSIONS

It has been hypothesized that the psychophysical detection of sinewave gratings is governed by *transient* mechanisms at low spatial frequencies and *sustained* mechanisms at high spatial frequencies. The former respond to temporal changes, and the latter respond to steady state signals.

In the first of two experiments, this hypothesis was tested in two ways. Using a forced choice procedure, threshold contrasts for two subjects were measured at 6 spatial frequencies and 10 durations, in the presence or absence of brief, masking gratings.

(1) In the absence of masking, the curves for threshold as a function of duration were of two types. For signals below 1.5 c/deg, threshold became independent of duration after a critical period of no more than 100 msec. For signals of 1.5 c/deg and above, the threshold curves exhibited an initial decline like those for lower spatial frequencies, but also a shallower secondary decline to an asymptotic level. The results are those predicted for the sustained/transient dichotomy. At all frequencies, the initial decline had a log-log slope near -0.7 , and at high spatial frequencies, the secondary decline has a slope near -0.3 .

(2) The high contrast masking gratings were 20 msec pulses which masked the onset and offset of the signal gratings. At 1.5 c/deg and above, masked threshold curves showed a regular decline to an asymptotic level equal to that of the unmasked curve. This result is consistent with the hypothesis of sustained response at high spatial frequencies. Below 1.5 c/deg, the threshold curves also showed a steady decline for at least 1000 msec, a characteristic typical of sustained response. It was hypothesized, therefore, that masking had desensitized the low frequency transient mechanisms, rendering them less sensitive than coexisting sustained mechanisms. This hypothesis was supported by a control experiment in which lower contrast masking of 0.375 c/deg signals yielded an elevated threshold curve of the shape predicted for transient response.

In the second experiment, the masking procedure was used to obtain spatial frequency bandwidths. Thresholds for 6 sinewave grating signals were measured as a function of the spatial frequency of the masking pulses.

(1) For spatial frequencies of 3.0, 6.0 and 12.0 c/deg, the bandwidth functions peaked at the signal frequencies, were of medium bandwidth (1–2 octaves), and were slightly skewed in shape.

(2) The bandwidth functions for signals of 1.5, 0.75 and 0.375 c/deg all peaked near 1.0–1.5 c/deg. Below the peak, the bandwidth functions for lower frequency signals were of greater magnitude. These character-

istics of the bandwidth functions suggested that low frequency signal detection under masked conditions was due to a sustained mechanism with optimal sensitivity near 1.5 c/deg. In a control experiment, the bandwidth function for a 1000 msec signal of 0.375 c/deg was measured. The resulting function was nearly constant from 0.27–3.0 c/deg with a value near 3.0 decilogs, indicating that transient detection at 0.375 c/deg can be masked by stimuli 3–4 octaves higher in spatial frequency.

The combined results of the two experiments confirm that transient and sustained mechanisms operate at low and high frequencies respectively. They also suggest that coexisting sustained mechanisms function at low frequencies as well, but manifest their presence in threshold detection only when the transient mechanisms have been desensitized.

Acknowledgements—I wish to thank Dr. R. J. W. Mansfield, Prof. David M. Green, and Dr. C. F. Stromeyer III for their very helpful comments, suggestions, and criticisms. I also wish to thank John Daugman and Wendy Willson Legge for their many hours of careful observations. I am grateful to Scott Bradner, manager of the Computer Based Laboratory. He designed and constructed the circuitry necessary to produce the displays, and helped with many other computer related problems. I thank the National Research Council of Canada for a postgraduate scholarship. The work was supported in part by a Grant-in-Aid of Research from the Society of Sigma Xi to the author, and by NSF research grant BNS75-08437 to Dr. Mansfield. The experiments reported in this paper formed part of a doctoral dissertation submitted to Harvard University. This paper was completed at the Physiological Laboratory, University of Cambridge, with the support of a Medical Research Council of Canada postdoctoral fellowship.

REFERENCES

- Arend L. E. Jr. (1976a) Response of the human eye to spatially sinusoidal gratings at various exposure durations. *Vision Res.* **16**, 1311–1317.
- Arend L. E. Jr. (1976b) Temporal determinants of the form of the spatial contrast threshold MTF. *Vision Res.* **16**, 1035–1041.
- Barlow H. B. (1958) Temporal and spatial summation in human vision at different background intensities. *J. Physiol., Lond.* **141**, 337–350.
- Baron W. and Westheimer G. (1973) Visual acuity as a function of exposure duration. *J. opt. Soc. Am.* **63**, 212–219.
- Blackwell H. R. (1946) Contrast thresholds of the human eye. *J. opt. Soc. Am.* **36**, 624–643.
- Blackwell H. R. (1963) Neural theories of simple visual discrimination. *J. opt. Soc. Am.* **53**, 129–160.
- Blakemore C. and Campbell F. W. (1969) On the existence of neurones in the human visual system selectively sensitive to the orientation and size of retinal images. *J. Physiol., Lond.* **203**, 237–260.
- Blakemore C. and Sutton P. (1969) Size adaptation: a new aftereffect. *Science, N.Y.* **166**, 245–247.
- Boycoff B. B. and Wässle H. (1974) The morphological types of ganglion cells of the domestic cat's retina. *J. Physiol., Lond.* **240**, 397–419.
- Breitmeyer B. G. (1975) Simple reaction time as a measure of the temporal response properties of transient and sustained channels. *Vision Res.* **15**, 1411–1412.
- Breitmeyer B. G. and Ganz L. (1977) Temporal studies with flashed gratings: inferences about human transient and sustained systems. *Vision Res.* **17**, 861–865.
- Breitmeyer B. G. and Julesz B. (1975) The role of on and off transients in determining the psychophysical spatial frequency response. *Vision Res.* **15**, 411–415.
- Brown J. L. and Black J. (1976) Critical duration for resolution of acuity targets. *Vision Res.* **16**, 309–315.
- Campbell F. W. (1974) The transmission of spatial information through the visual system. In *The Neurosciences Third Study Program* (Edited by Schmitt F. O. and Worden F. G.), pp. 95–103. MIT Press, Cambridge, Mass.
- Campbell F. W. and Green D. G. (1965) Optical and retinal factors affecting visual resolution. *J. Physiol., Lond.* **181**, 576–593.
- Campbell F. W. and Kulikowski J. J. (1966) Orientational selectivity of the human visual system. *J. Physiol., Lond.* **187**, 437–445.
- Campbell F. W. and Robson J. G. (1968) Application of Fourier analysis to the visibility of gratings. *J. Physiol., Lond.* **197**, 551–566.
- Cleland B., Dubin M. W. and Levick W. R. (1971) Sustained and transient neurones in the cat's retina and lateral geniculate nucleus. *J. Physiol., Lond.* **217**, 473–496.
- Cleland B., Levick W. R. and Sanderson K. J. (1973) Properties of sustained and transient ganglion cells in the cat retina. *J. Physiol., Lond.* **228**, 649–680.
- Enroth-Cugell C. and Robson J. G. (1966) The contrast sensitivity of retinal ganglion cells of the cat. *J. Physiol., Lond.* **187**, 517–552.
- Fiorentini A. and Maffei L. (1976) Spatial contrast sensitivity of myopic subjects. *Vision Res.* **16**, 437–438.
- Graham C. H. and Kemp E. H. (1938) Brightness discrimination as a function of the duration of the increment in intensity. *J. gen. Physiol.* **24**, 635–650.
- Green D. M. and Luce R. D. (1975) Parallel psychometric functions from a set of independent detectors. *Psychol. Rev.* **82**, 483–486.
- Gouras P. (1969) Antidromic responses of orthodromically identified ganglion cells in monkey retina. *J. Physiol., Lond.* **204**, 407–419.
- Hochstein S. and Shapley R. M. (1976a) Linear and non-linear spatial subunits in Y cat retinal ganglion cells. *J. Physiol., Lond.* **262**, 265–284.
- Hochstein S. and Shapley R. M. (1976b) Quantitative analysis of retinal ganglion cell classifications. *J. Physiol., Lond.* **262**, 237–264.
- Ikeda H. and Wright M. J. (1972) Receptive field organization of 'sustained' and 'transient' retinal ganglion cells which subserve different functional roles. *J. Physiol., Lond.* **227**, 769–800.
- Ikeda H. and Wright M. J. (1975) Spatial and temporal properties of sustained and transient neurones in area 17 of the cat's visual cortex. *Expl Brain Res.* **222**, 363–383.
- Kahneman D. (1964) Temporal summation in an acuity task at different energy levels: a study of the determinants of summation. *Vision Res.* **4**, 557–576.
- Keesey U. T. (1960) Effect of involuntary eye movements on visual acuity. *J. opt. Soc. Am.* **50**, 769–774.
- Keesey U. T. (1972) Flicker and pattern detection: a comparison of thresholds. *J. opt. Soc. Am.* **62**, 446–448.
- Kelly D. H. (1971) Theory of flicker and transient response. II: counterphase gratings. *J. opt. Soc. Am.* **61**, 632–640.
- King-Smith P. E. and Kulikowski J. J. (1975) Pattern and flicker detection analyzed by subthreshold summation. *J. Physiol., Lond.* **249**, 519–549.
- Kulikowski J. J. (1971) Some stimulus parameters affecting spatial and temporal resolution of human vision. *Vision Res.* **11**, 83–90.
- Kulikowski J. J. and Tolhurst D. J. (1973) Psychophysical evidence for sustained and transient detectors in human vision. *J. Physiol., Lond.* **232**, 149–162.

- Levick W. R. (1974) Form and function of cat retinal ganglion cells. *Nature*, **254**, 659–662.
- Lovegrove W. J. and Over R. (1972) Color adaptation of spatial frequency detectors in the human visual system. *Science*, N.Y. **176**, 541–543.
- Lupp U., Hauske G. and Wolf W. (1976) Perceptual latencies to sinusoidal gratings. *Vision Res.* **16**, 969–972.
- Mansfield R. J. W. (1973a) Brightness function: effect of area and duration. *J. opt. Soc. Am.* **63**, 913–920.
- Mansfield R. J. W. (1973b) Latency functions in human vision. *Vision Res.* **13**, 2219–2234.
- Marrocco R. T. (1976) Sustained and transient cells in monkey lateral geniculate nucleus: conduction velocities and response properties. *J. Neurophysiol.* **39**, 340–353.
- Movshon J. H. and Blakemore C. (1973) Orientation specificity and spatial selectivity in human vision. *Perception*, **2**, 53–60.
- Nachmias J. (1967) The effect of exposure duration on visual contrast sensitivity with square-wave gratings. *J. opt. Soc. Am.* **57**, 421–427.
- Nachmias J. and Weber A. (1975) Discrimination of simple and complex gratings. *Vision Res.* **15**, 217–223.
- Pantle A. and Sekuler R. (1968) Size detecting mechanisms in human vision. *Science*, N.Y. **162**, 1146–1148.
- Riggs L. A., Armington J. C. and Ratliff F. (1954) Motions of the retinal image during fixation. *J. opt. Soc. Am.* **44**, 315–321.
- Sachs M. B., Nachmias J. and Robson J. G. (1971) Spatial frequency channels in human vision. *J. opt. Soc. Am.* **61**, 1176–1186.
- Schober H. A. W. and Hilz R. (1965) Contrast sensitivity of the human eye for square-wave gratings. *J. opt. Soc. Am.* **55**, 1086–1091.
- Scobey R. P. and Horowitz J. M. (1976) Detection of image displacement by phasic cells in peripheral visual fields of the monkey. *Vision Res.* **16**, 15–24.
- Sharpe C. R. (1974) The color specificity of spatial adaptation, red–blue interactions. *Vision Res.* **14**, 41–51.
- Sherman S. M., Wilson J. R., Kaas J. H. and Webb S. V. X- and Y-cells in the dorsal lateral geniculate nucleus of the owl monkey (*Aotus trivirgatus*). *Science*, N.Y. **192**, 475–477.
- Spitzberg R. and Richards W. (1975) Broad band spatial filters in the human visual system. *Vision Res.* **15**, 837–841.
- Stromeyer C. F. III and Julesz B. (1972) Spatial frequency masking in vision: critical bands and spread of masking. *J. opt. Soc. Am.* **62**, 1221–1232.
- Stromeyer C. F. III and Klein S. (1974) Spatial frequency channels in human vision as asymmetrical (edge) mechanisms. *Vision Res.* **14**, 1409–1420.
- Stromeyer C. F. III, Spillmann L., Klein S. and Dawson B. M. (1976) Adaptation to low spatial frequencies: movement or form channels? Unpublished manuscript.
- Tolhurst D. J. (1973) Separate channels for the analysis of the shape and the movement of a moving visual stimulus. *J. Physiol., Lond.* **231**, 385–402.
- Tolhurst D. J. (1975a) Reaction times in the detection of gratings by human observers: a probabilistic mechanism. *Vision Res.* **15**, 1143–1150.
- Tolhurst D. J. (1975b) Sustained and transient channels in human vision. *Vision Res.* **15**, 1151–1155.
- Tolhurst D. J., Sharpe C. and Hart G. (1973) The analysis of the drift rate of moving sinusoidal gratings. *Vision Res.* **13**, 2545–2555.
- Tulunay-Keesey U. and Jones R. M. (1976) The effect of micromovements of the eye and the exposure duration on contrast sensitivity. *Vision Res.* **16**, 481–488.
- van Nes F. L., Koenderink J. J., Nas H. and Bouman M. A. (1967) Spatio-temporal modulation transfer in the human eye. *J. opt. Soc. Am.* **57**, 1082–1088.
- Vassilev A. and Mitov D. (1976) Perception time and spatial frequency. *Vision Res.* **16**, 89–92.
- Wetherill G. B. and Levitt H. (1964) Sequential estimation of points on a psychometric function. *Br. J. math. Stat. Psychol.* **18**, 1–10.

APPENDIX: PROOF OF EQUATION (5)

Assume an interval t , is divided into N equal intervals. Let the probability of detection in any interval be a function of a parameter R . The probability of detection in the i th interval is $P_i(R)$ and the probability of no detection is $Q_i(R) = 1 - P_i(R)$. Suppose that detection in the N intervals is independent. Then, the overall probability of no detection Q_0 is:

$$Q_0 = \prod_{i=1}^N Q_i(R)$$

If R is constant, and independent of time, all the values of Q_i are equal, and may be denoted $Q_N(R)$. Also, Q_0 may be regarded as a function of R :

$$Q_0(R) = \prod_{i=1}^N Q_N(R) = Q_N(R)^N$$

Therefore:

$$Q_N(R) = Q_0(R)^{1/N}$$

Now, suppose R is a function of time t :

$$Q_0 = \prod_{i=1}^N Q_i(R(t)) = \prod_{i=1}^N Q_{0i}(R(t))^{1/N}$$

where Q_{0i} is the value of Q_0 which would be obtained if R were constant at the value $R(t)$ for the entire interval. Taking logs of both sides:

$$\ln Q_0 = \frac{1}{N} \sum_{i=1}^N \ln Q_{0i}(R(t)) = \frac{1}{N} \sum_{i=1}^N \ln [1 - P_{0i}(R(t))]$$

Let the summation pass to an integral by allowing $N \rightarrow \infty$ and by making $P_{0i}(R(t))$ contract to a density function $f(t)$. Then:

$$\ln Q_0 = \int_0^{t_0} \ln [1 - f(t)] dt$$

$$Q_0 = \exp \left\{ \int_0^{t_0} \ln [1 - f(t)] dt \right\}$$

Finally, the total probability of detection in the interval is:

$$P_0 = 1 - Q_0 = 1 - \exp \left\{ \int_0^{t_0} \ln [1 - f(t)] dt \right\}$$

This is equation (5).